QUATERNION-BASED WORST CASE CONSTRAINED BEAMFORMER BASED ON ELECTROMAGNETIC VECTOR-SENSOR ARRAYS

Xirui Zhang[⋆†] *Wei Liu*[†] *Yougen Xu*[⋆] *Zhiwen Liu*[⋆]

[⋆] School of Information and Electronics
Beijing Institute of Technology, Beijing, 100081, China

[†] Communications Research Group
Department of Electronic and Electrical Engineering
University of Sheffield, Sheffield, S1 3JD, United Kingdom

xi-rui.zhang@sheffield.ac.uk

ABSTRACT

A robust adaptive beamforming scheme based on two-component electromagnetic (EM) vector-sensor arrays is proposed by extending the well-known worst-case constraint into the quaternionic domain. After defining the uncertainty set of the desired signal's quaternionic steering vector, two quaternion-based constrained minimization problems are derived. We then reformulate them into two real-valued convex quadratic problems, which can be easily solved via the second-order cone (SOC) programming approach. Numerical simulations show that our quaternion-based robust beamformer significantly outperforms the sample matrix inversion minimum variance distortionless response (SMI-MVDR) beamformer and the quaternion Capon (Q-Capon) beamformer in the presence of steering vector mismatches.

Index Terms— Robust adaptive beamformer, vector-sensor array, quaternion, worst case constraint.

1. INTRODUCTION

Adaptive beamforming with EM vector-sensor arrays can exploit not only the directions of arrival (DOAs) of the impinging signals but also their polarizations. The so-called crossed-dipole and tripole (the earliest EM vector-sensors, known as 'polarization diverse antennas') were first introduced into the field of adaptive arrays in [1, 2]. Based on such a system, the adaptive beamforming problem was studied in detail in terms of the output signal-to-interference-plus-noise ratio (SINR) in [3]. Furthermore, it was shown that a 'complete' EM vector-sensor (measuring the six components of an EM field at the same point) with identical electric and magnetic noise power can eliminate the angular grating nulls completely. Moreover, with the analysis in [4], it was concluded that the output SINR is determined by both DOA and polarization differences of the impinging signals in the case of unequal noise power.

The above methods assume an exactly known steering vector for the desired signal. When the estimation of the steering vector is imprecise, especially with look direction and sensor position errors, the performance of conventional MVDR beamformers will deteriorate. To enhance its robustness, many methods have been proposed, such as diagonal loading [5], and the approach based on the optimization of worst case performance [6, 7, 8, 9, 10, 11, 12]. In particular, the worst-case constrained beamformer (WCCB) can be considered as one specific type of the diagonal-loading scheme, where the loading factor is determined based on the known level of uncertainty of the desired signal's steering vector.

Very recently, improved robustness against steering vector mismatch error has been shown by quaternion formulation. The quaternionic model of a two-component vector-sensor array was firstly provided in [13, 14], and a multiple signal classification (MUSIC)-like scheme was applied accordingly. In adaptive beamforming, the quaternionic version of the conventional MVDR beamformer has been derived with a two-component EM vector-sensor array in [15, 16], where a better performance is obtained in the presence of steering vector mismatch error. However, the well-known WCCB has not been investigated in the hypercomplex domain yet. Therefore, a novel quaternionic adaptive beamformer based on the worst-case constraint is proposed here to tackle the steering vector mismatch problem. Two adaptive algorithms are derived in detail and as will be shown in our simulations, they significantly outperform both the SMI-MVDR beamformer [17], and the Q-Capon beamformer [15].

The rest of this paper is organized as follows. Section 2 introduces the quaternion-based signal model for a two-component EM vector-sensor array, and gives the theoretical derivation of the two proposed algorithms. Numerical simulations are provided in Section 3, and conclusions are drawn in Section 4.

2. THE PROPOSED QUATERNIONIC BEAMFORMER WITH WORST-CASE CONSTRAINT

2.1. Quaternions

A quaternion $q \in \mathbb{H}^1$ ($\mathbb{R}, \mathbb{C}$, and $\mathbb{H}$ denote the sets of real numbers, complex numbers and quaternions, respectively), is defined as

$$q \triangleq q_0 + q_1\mathrm{i} + q_2\mathrm{j} + q_3\mathrm{k}\ , \tag{1}$$

where $q_0 \triangleq \mathrm{Re}\{q\} \in \mathbb{R}$ is the real component, and $q_1 \triangleq \mathrm{Im}^{(1)}\{q\}$, $q_2 \triangleq \mathrm{Im}^{(2)}\{q\}$, $q_3 \triangleq \mathrm{Im}^{(3)}\{q\} \in \mathbb{R}$ are the three imaginary components, with units i, j, and k satisfying

$$\begin{gathered}\mathrm{ii} = \mathrm{jj} = \mathrm{kk} = -1,\\ \mathrm{ij} = -\mathrm{ji} = \mathrm{k};\ \mathrm{jk} = -\mathrm{kj} = \mathrm{i};\ \mathrm{ki} = -\mathrm{ik} = \mathrm{j}.\end{gathered} \tag{2}$$

Similarly, for a vector $\mathbf{v} \in \mathbb{H}^{L_1 \times 1}$ and a matrix $\mathbf{M} \in \mathbb{H}^{L_1 \times L_2}$, we have

$$\mathbf{v} \triangleq \mathbf{v}_0 + \mathbf{v}_1\mathrm{i} + \mathbf{v}_2\mathrm{j} + \mathbf{v}_3\mathrm{k},$$
$$\mathbf{M} \triangleq \mathbf{M}_0 + \mathbf{M}_1\mathrm{i} + \mathbf{M}_2\mathrm{j} + \mathbf{M}_3\mathrm{k}, \tag{3}$$

where $\mathbf{v}_l \in \mathbb{R}^{L_1 \times 1}$, and $\mathbf{M}_l \in \mathbb{R}^{L_1 \times L_2}$, $l = 0, \cdots, 3$. Three properties used in this paper are introduced as follows. More details can be found in [18].

Property 1. Given $\mathbf{M} \in \mathbb{H}^{L_1 \times L_2}$ and $\mathbf{v} \in \mathbb{H}^{L_2 \times 1}$, we have

$$(\mathbf{M}\mathbf{v})^{\triangleleft} = \mathbf{v}^{\triangleleft}\mathbf{M}^{\triangleleft} , \tag{4}$$

where '$\{\}^{\triangleleft}$' denotes the conjugate transpose of quaternionic matrices and vectors [18].

Property 2. For a conjugate symmetric quaternionic matrix $\mathbf{M} \in \mathbb{H}^{L_1 \times L_2}$ and a quaternionic vector $\mathbf{v} \in \mathbb{H}^{L_1 \times 1}$, we have

$$\mathbf{v}^{\triangleleft}\mathbf{M}\mathbf{v} = \mathbf{v}_1^{\triangleleft}\mathbf{M}\mathbf{v}_1, \quad \text{with } \mathbf{v}_1 = \mathbf{v} \cdot \mathrm{e}^{\epsilon\vartheta} , \tag{5}$$

where

$$\epsilon = \frac{q_1\mathrm{i} + q_2\mathrm{j} + q_3\mathrm{k}}{\sqrt{q_1^2 + q_2^2 + q_3^2}}, \;\; \vartheta = \arctan\left(\sqrt{q_1^2 + q_2^2 + q_3^2}/q_0\right). \tag{6}$$

Property 3. The Euclidean-norm of two quaternionic vectors $\mathbf{a}, \mathbf{b} \in \mathbb{H}^{L_1 \times 1}$, satisfies the following two inequalities [19]

$$\|\mathbf{a} + \mathbf{b}\| \geq \|\mathbf{a}\| - \|\mathbf{b}\|, \;\; |\mathbf{a}^{\triangleleft}\mathbf{b}| \leq \|\mathbf{a}\|\|\mathbf{b}\|. \tag{7}$$

2.2. Quaternion-based Signal Model

Consider a uniform linear array (ULA) consisting of N crossed-dipoles (the typical two-component EM vector-sensor) located along the y-axis with an adjacent sensor spacing d. As shown in Fig. 1, the two components of each crossed-dipole are parallel to $x-$ and $y-$ axes, respectively. Suppose there are M uncorrelated narrowband far-field signals $\{s_m(t)\}_{m=1}^M$ impinging upon the array from the $y-z$ plane with DOA angles $(\theta_1, \cdots, \theta_M) \in [0, \pi]$. All the incident signals have the same wavelength λ_0. Then, the spatial steering vector for the mth signal can be expressed as

$$\mathbf{a}_{\mathrm{s},m} = \left[1, e^{-\mathrm{j}\frac{2\pi d \sin\theta_m}{\lambda_0}}, \cdots, e^{-\mathrm{j}\frac{2\pi(N-1)d\sin\theta_m}{\lambda_0}}\right]^{\mathrm{T}}, \tag{8}$$

where '$\{\}^{\mathrm{T}}$' denotes the transpose operation. For a crossed-dipole, the spatial-polarization coherent vector of the mth signal with auxiliary polarization angle $\gamma_m \in [0, \pi/2]$ and polarization phase difference $\eta_m \in [-\pi, \pi)$, can be written as

$$\mathbf{a}_{\mathrm{p},m} = \left[-\cos\gamma_m, \cos\theta_m \sin\gamma_m e^{\mathrm{j}\eta_m}\right]^{\mathrm{T}}. \tag{9}$$

Now, we divide the ULA into two subarrays: one is composed of all the dipoles pointing along the $x-$axis, while the other includes all the dipoles along the $y-$axis. Then, their steering vectors $\mathbf{a}_{\mathrm{x},m} \in \mathbb{C}^{N \times 1}$ and $\mathbf{a}_{\mathrm{y},m} \in \mathbb{C}^{N \times 1}$ for the mth signal are

$$\mathbf{a}_{\mathrm{x},m} = -\cos\gamma_m \cdot \mathbf{a}_{\mathrm{s},m}, \;\; \mathbf{a}_{\mathrm{y},m} = \cos\theta_m \sin\gamma_m e^{\mathrm{j}\eta_m} \cdot \mathbf{a}_{\mathrm{s},m}. \tag{10}$$

The outputs of these two subarrays can be written as

$$\mathbf{x}(t) = \sum_{m=1}^{M} \mathbf{a}_{\mathrm{x},m} s_m(t) + \mathbf{n}_{\mathrm{x}}(t), \tag{11}$$

$$\mathbf{y}(t) = \sum_{m=1}^{M} \mathbf{a}_{\mathrm{y},m} s_m(t) + \mathbf{n}_{\mathrm{y}}(t), \tag{12}$$

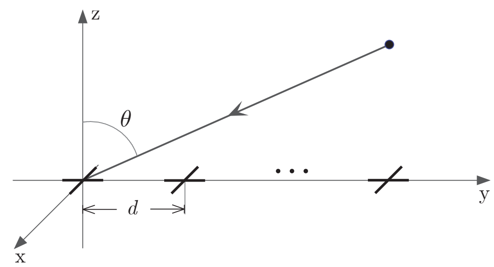

Fig. 1. A ULA with crossed-dipoles.

where $\mathbf{n}_{\mathrm{x}}(t)$ and $\mathbf{n}_{\mathrm{y}}(t) \in \mathbb{C}^{N \times 1}$ denote the corresponding additive white Gaussian noise vectors.

Thus, the quaternionic output vector $\mathbf{q}(t) \in \mathbb{H}^{N \times 1}$ of the crossed-dipole-based ULA can be defined as

$$\mathbf{q}(t) \triangleq \mathbf{x}(t) + \mathrm{i}\mathbf{y}(t) = \sum_{m=1}^{M} \mathbf{a}_m s_m(t) + \mathbf{n}(t) , \tag{13}$$

where $\mathbf{a}_m \triangleq \mathbf{a}_{\mathrm{x},m} + \mathrm{i}\mathbf{a}_{\mathrm{y},m} \in \mathbb{H}^{N \times 1}$ is the quaternionic steering vector, and $\mathbf{n}(t) \triangleq \mathbf{n}_{\mathrm{x}} + \mathrm{i}\mathbf{n}_{\mathrm{y}} \in \mathbb{H}^{N \times 1}$ the quaternionic noise vector. Given the k-th snapshot data $\mathbf{q}[k] \in \mathbb{H}^{N \times 1}$ of $\mathbf{q}(t)$, the sample quaternionic covariance matrix $\hat{\mathbf{R}} \in \mathbb{H}^{N \times N}$ can be obtained by

$$\hat{\mathbf{R}} = \frac{1}{K}\sum_{k=1}^{K} \mathbf{q}[k]\mathbf{q}^{\triangleleft}[k]. \tag{14}$$

2.3. Steering Vector Model

Assume that one of the M incident array signals is the desired one and its presumed quaternionic steering vector is denoted as $\bar{\mathbf{a}}_{\mathrm{d}} \in \mathbb{H}^{N \times 1}$. With steering vector mismatch, there will be a non-zero quaternionic error vector $\mathbf{e} \in \mathbb{H}^{N \times 1}$ between $\bar{\mathbf{a}}_{\mathrm{d}}$ and the actual steering vector $\mathbf{a}_{\mathrm{d}} \in \mathbb{H}^{N \times 1}$, i.e.

$$\mathbf{a}_{\mathrm{d}} = \bar{\mathbf{a}}_{\mathrm{d}} + \mathbf{e} . \tag{15}$$

We assume that its norm is bounded by a real positive constant ε, i.e. $\|\mathbf{e}\| \leq \varepsilon$. Then, the actual steering vector $\mathbf{a}_{\mathrm{d}}$ can be modelled as belonging to a steering vector set $\mathcal{A}$ defined by

$$\mathcal{A} \triangleq \left\{\mathbf{a}_{\mathrm{d}} | \mathbf{a}_{\mathrm{d}} = \bar{\mathbf{a}}_{\mathrm{d}} + \mathbf{e}, \|\mathbf{e}\| \leq \varepsilon\right\}. \tag{16}$$

From (16), we can see that $\mathcal{A}$ is a spherical set where $\bar{\mathbf{a}}_{\mathrm{d}}$ is in the center, whilst $\mathbf{a}_{\mathrm{d}}$ can be any vector in $\mathcal{A}$.

2.4. Quaternion-based Worst-case Constrained Algorithm 1

Since $\mathbf{a}_{\mathrm{d}}$ can be any vector in $\mathcal{A}$, in order to have a robust response to the desired signal, we can impose the following constraint to the weight vector $\mathbf{w} \in \mathbb{H}^{N \times 1}$

$$\min_{\mathbf{a}_{\mathrm{d}} \in \mathcal{A}} |\mathbf{w}^{\triangleleft}\mathbf{a}_{\mathrm{d}}| \geq 1 , \tag{17}$$

which is referred to as the quaternionic worst-case constraint. Under such a constraint, the magnitude of the array response for all the steering vectors in set $\mathcal{A}$ is constrained to be greater than unity.

By adopting (17), a novel robust adaptive beamformer, named quaternionic beamformer with worst-case constraint, can be formulated as follows

$$\min_{\mathbf{w}} \mathbf{w}^{\triangleleft}\hat{\mathbf{R}}\mathbf{w} \quad \text{s.t.} \quad \min_{\mathbf{a}_{\mathrm{d}} \in \mathcal{A}} |\mathbf{w}^{\triangleleft}\mathbf{a}_{\mathrm{d}}| \geq 1 \tag{18}$$

where $\hat{\mathbf{R}}$ is the sample quaternionic covariance matrix obtained by (14). In the next, we will reformulate the problem in (18), so that it can be solved by SOC programming based approach.

Firstly, using the triangle inequality property in (7), we have

$$|\mathbf{w}^{\triangleleft}\mathbf{a}_{\mathrm{d}}| = |\mathbf{w}^{\triangleleft}\bar{\mathbf{a}}_{\mathrm{d}} + \mathbf{w}^{\triangleleft}\mathbf{e}| \geq |\mathbf{w}^{\triangleleft}\bar{\mathbf{a}}_{\mathrm{d}}| - |\mathbf{w}^{\triangleleft}\mathbf{e}|. \tag{19}$$

Applying the Cauchy's inequality in (7) to $|\mathbf{w}^{\triangleleft}\mathbf{e}|$ and with $\|\mathbf{e}\| \leq \varepsilon$, we further have

$$|\mathbf{w}^{\triangleleft}\mathbf{e}| \leq \|\mathbf{w}\|\|\mathbf{e}\| \leq \varepsilon\|\mathbf{w}\|. \tag{20}$$

Combining (19) and (20) leads to

$$|\mathbf{w}^{\triangleleft}\mathbf{a}_{\mathrm{d}}| \geq |\mathbf{w}^{\triangleleft}\bar{\mathbf{a}}_{\mathrm{d}}| - \varepsilon\|\mathbf{w}\|. \tag{21}$$

As a result, the constrained minimization problem in (18) can be transformed into

$$\min_{\mathbf{w}} \mathbf{w}^{\triangleleft}\hat{\mathbf{R}}\mathbf{w} \quad \text{s.t.} \quad |\mathbf{w}^{\triangleleft}\bar{\mathbf{a}}_{\mathrm{d}}| \geq 1 + \varepsilon\|\mathbf{w}\|. \tag{22}$$

However, due to the absolute operation in the constraint, (22) is still a nonconvex problem. According to property 2 in (5), the beamformer's output power $\mathbf{w}^{\triangleleft}\hat{\mathbf{R}}\mathbf{w}$ would not be changed if the quaternionic vector $\mathbf{w}$ undergoes an arbitrary phase shift. For a given level of $\mathbf{w}^{\triangleleft}\hat{\mathbf{R}}\mathbf{w}$, we can change the phase of $\mathbf{w}$ without affecting $|\mathbf{w}^{\triangleleft}\bar{\mathbf{a}}_{\mathrm{d}}|$. Multiplying the weight vector $\mathbf{w}$ by an appropriate phase factor, we can always make $\mathbf{w}^{\triangleleft}\bar{\mathbf{a}}_{\mathrm{d}}$ a real value, whilst keeping the output power unchanged. Then the constraint in (22) can be rewritten as

$$\begin{aligned} &\mathrm{Re}\{\mathbf{w}^{\triangleleft}\bar{\mathbf{a}}_{\mathrm{d}}\} \geq 1 + \varepsilon\|\mathbf{w}\|,\ \mathrm{Im}^{(1)}\{\mathbf{w}^{\triangleleft}\bar{\mathbf{a}}_{\mathrm{d}}\} = 0, \\ &\mathrm{Im}^{(2)}\{\mathbf{w}^{\triangleleft}\bar{\mathbf{a}}_{\mathrm{d}}\} = 0,\ \mathrm{Im}^{(3)}\{\mathbf{w}^{\triangleleft}\bar{\mathbf{a}}_{\mathrm{d}}\} = 0. \end{aligned} \tag{23}$$

Thus, the constrained minimization problem in (22) can be reformulated into a convex quadratic problem as follows

$$\begin{aligned} \min_{\mathbf{w}} \mathbf{w}^{\triangleleft}\hat{\mathbf{R}}\mathbf{w} \quad \text{s.t.} \quad &\mathrm{Re}\{\mathbf{w}^{\triangleleft}\bar{\mathbf{a}}_{\mathrm{d}}\} \geq 1 + \varepsilon\|\mathbf{w}\|, \\ &\mathrm{Im}^{(1)}\{\mathbf{w}^{\triangleleft}\bar{\mathbf{a}}_{\mathrm{d}}\} = 0,\ \mathrm{Im}^{(2)}\{\mathbf{w}^{\triangleleft}\bar{\mathbf{a}}_{\mathrm{d}}\} = 0, \\ &\mathrm{Im}^{(3)}\{\mathbf{w}^{\triangleleft}\bar{\mathbf{a}}_{\mathrm{d}}\} = 0. \end{aligned} \tag{24}$$

We refer to the above formulation as the quaternion worst-case constrained beamformer 1 (Q-WCCB-1).

2.5. Quaternion-based Worst-case Constrained Algorithm 2

Following the argument after (22), in the second algorithm, instead of imposing the constraint on the absolute value of $\mathbf{w}^{\triangleleft}\mathbf{a}_{\mathrm{d}}$, the worst case constraint is imposed on the real component of $\mathbf{w}^{\triangleleft}\mathbf{a}_{\mathrm{d}}$, given as

$$\min_{\mathbf{w}} \mathbf{w}^{\triangleleft}\hat{\mathbf{R}}\mathbf{w} \quad \text{s.t.} \quad \min_{\mathbf{a}_{\mathrm{d}} \in \mathcal{A}} \mathrm{Re}\{\mathbf{w}^{\triangleleft}\mathbf{a}_{\mathrm{d}}\} \geq 1. \tag{25}$$

Using (15), we have

$$\mathrm{Re}\{\mathbf{w}^{\triangleleft}\mathbf{a}_{\mathrm{d}}\} \geq \mathrm{Re}\{\mathbf{w}^{\triangleleft}\bar{\mathbf{a}}_{\mathrm{d}}\} - |\mathbf{w}^{\triangleleft}\mathbf{e}| \geq \mathrm{Re}\{\mathbf{w}^{\triangleleft}\bar{\mathbf{a}}_{\mathrm{d}}\} - \varepsilon\|\mathbf{w}\|. \tag{26}$$

Then, the constraint in (25) can be replaced by

$$\mathrm{Re}\{\mathbf{w}^{\triangleleft}\bar{\mathbf{a}}_{\mathrm{d}}\} - \varepsilon\|\mathbf{w}\| \geq 1. \tag{27}$$

The problem (25) can therefore be reformulated into

$$\min_{\mathbf{w}} \mathbf{w}^{\triangleleft}\hat{\mathbf{R}}\mathbf{w} \quad \text{s.t.} \quad \mathrm{Re}\{\mathbf{w}^{\triangleleft}\bar{\mathbf{a}}_{\mathrm{d}}\} \geq 1 + \varepsilon\|\mathbf{w}\|, \tag{28}$$

We refer to (28) as the quaternion worst-case constrained beamformer 2 (Q-WCCB-2).

2.6. SOC Implementation of Q-WCCB-1 and Q-WCCB-2

The constrained minimization problems in (24) and (28) can be solved by the SOC programming method. A SOC program is a convex optimization problem with the form as

$$\min \mathbf{f}^{\mathrm{T}}\mathbf{x} \quad \text{s.t.} \quad \|\mathbf{A}_i\mathbf{x} + \mathbf{b}_i\| \leq \mathbf{c}_i^{\mathrm{T}}\mathbf{x} + d_i, i = 1, ..., I \tag{29}$$

where $\mathbf{x} \in \mathbb{R}^{N\times 1}$ is the optimization variable, $\mathbf{f} \in \mathbb{R}^{N\times 1}$ denotes the known parameter vector, $\mathbf{A}_i \in \mathbb{R}^{N_i\times N}$, $\mathbf{b}_i \in \mathbb{R}^{N_i\times 1}$, $\mathbf{c}_i \in \mathbb{R}^{N_i\times 1}$, $d_i \in \mathbb{R}$, and I is the number of constraints.

Applying the Cholesky decomposition to $\hat{\mathbf{R}}$, we have

$$\hat{\mathbf{R}} = \mathbf{Q}^{\triangleleft}\mathbf{Q}\ , \tag{30}$$

where $\mathbf{Q} \in \mathbb{H}^{N\times N}$ is an upper triangular quaternionic matrix. Then the array's output power $\mathbf{w}^{\triangleleft}\hat{\mathbf{R}}\mathbf{w}$ can be rewritten as

$$\mathbf{w}^{\triangleleft}\hat{\mathbf{R}}\mathbf{w} = \mathbf{w}^{\triangleleft}\mathbf{Q}^{\triangleleft}\mathbf{Q}\mathbf{w} = (\mathbf{Q}\mathbf{w})^{\triangleleft}(\mathbf{Q}\mathbf{w}) = \|\mathbf{Q}\mathbf{w}\|^2. \tag{31}$$

Now, by adopting a new nonnegative scalar variable ξ and a new constraint $\|\mathbf{Q}\mathbf{w}\| \leq \xi$, the constrained minimization problems in (24) and (28) can be respectively transformed into

$$\begin{aligned} \min_{\mathbf{w},\xi} \xi \quad \text{s.t.} \quad &\|\mathbf{Q}\mathbf{w}\| \leq \xi,\ \varepsilon\|\mathbf{w}\| \leq \mathrm{Re}\{\mathbf{w}^{\triangleleft}\bar{\mathbf{a}}_{\mathrm{d}}\} - 1, \\ &\mathrm{Im}^{(1)}\{\mathbf{w}^{\triangleleft}\bar{\mathbf{a}}_{\mathrm{d}}\} = 0, \mathrm{Im}^{(2)}\{\mathbf{w}^{\triangleleft}\bar{\mathbf{a}}_{\mathrm{d}}\} = 0, \\ &\mathrm{Im}^{(3)}\{\mathbf{w}^{\triangleleft}\bar{\mathbf{a}}_{\mathrm{d}}\} = 0, \end{aligned} \tag{32}$$

and

$$\min_{\mathbf{w},\xi} \xi \quad \text{s.t.} \quad \|\mathbf{Q}\mathbf{w}\| \leq \xi,\ \varepsilon\|\mathbf{w}\| \leq \mathrm{Re}\{\mathbf{w}^{\triangleleft}\bar{\mathbf{a}}_{\mathrm{d}}\} - 1. \tag{33}$$

Note that the elements of $\mathbf{Q}$, $\mathbf{w}$ and $\bar{\mathbf{a}}_{\mathrm{d}}$ are quaternions. To facilitate the solution of (32) and (33), we need to convert them into real-valued forms. First of all, $\mathbf{Q}$, $\mathbf{w}$, $\bar{\mathbf{a}}_{\mathrm{d}}$ need to be written into the following forms

$$\begin{aligned} \mathbf{Q} &\triangleq \mathbf{Q}_0 + \mathbf{Q}_1\mathrm{i} + \mathbf{Q}_2\mathrm{j} + \mathbf{Q}_3\mathrm{k}, \\ \mathbf{w} &\triangleq \mathbf{w}_0 + \mathbf{w}_1\mathrm{i} + \mathbf{w}_2\mathrm{j} + \mathbf{w}_3\mathrm{k}, \\ \bar{\mathbf{a}}_{\mathrm{d}} &\triangleq \bar{\mathbf{a}}_{\mathrm{d},0} + \bar{\mathbf{a}}_{\mathrm{d},1}\mathrm{i} + \bar{\mathbf{a}}_{\mathrm{d},2}\mathrm{j} + \bar{\mathbf{a}}_{\mathrm{d},3}\mathrm{k}, \end{aligned} \tag{34}$$

where $\mathbf{Q}_l \in \mathbb{R}^{N\times N}$, $\mathbf{w}_l \in \mathbb{R}^{N\times 1}$, and $\bar{\mathbf{a}}_{\mathrm{d},l} \in \mathbb{R}^{N\times 1}$, $l = 0, 1, 2, 3$. Then, we further define one real-valued matrix and five real-valued vectors as follows

$$\begin{aligned} \breve{\mathbf{Q}} &\triangleq \begin{bmatrix} \mathbf{Q}_0 & -\mathbf{Q}_1 & -\mathbf{Q}_2 & -\mathbf{Q}_3 \\ \mathbf{Q}_1 & \mathbf{Q}_0 & -\mathbf{Q}_3 & \mathbf{Q}_2 \\ \mathbf{Q}_2 & \mathbf{Q}_3 & \mathbf{Q}_0 & -\mathbf{Q}_1 \\ \mathbf{Q}_3 & -\mathbf{Q}_2 & \mathbf{Q}_1 & \mathbf{Q}_0 \end{bmatrix}, \\ \breve{\mathbf{w}} &\triangleq \left[\mathbf{w}_0^{\mathrm{T}}, \mathbf{w}_1^{\mathrm{T}}, \mathbf{w}_2^{\mathrm{T}}, \mathbf{w}_3^{\mathrm{T}}\right]^{\mathrm{T}}, \\ \bar{\mathbf{a}}_{\mathrm{d}}^{(1)} &\triangleq \left[\bar{\mathbf{a}}_{\mathrm{d},0}^{\mathrm{T}}, \bar{\mathbf{a}}_{\mathrm{d},1}^{\mathrm{T}}, \bar{\mathbf{a}}_{\mathrm{d},2}^{\mathrm{T}}, \bar{\mathbf{a}}_{\mathrm{d},3}^{\mathrm{T}}\right]^{\mathrm{T}}, \\ \bar{\mathbf{a}}_{\mathrm{d}}^{(2)} &\triangleq \left[\bar{\mathbf{a}}_{\mathrm{d},1}^{\mathrm{T}}, -\bar{\mathbf{a}}_{\mathrm{d},0}^{\mathrm{T}}, -\bar{\mathbf{a}}_{\mathrm{d},3}^{\mathrm{T}}, \bar{\mathbf{a}}_{\mathrm{d},2}^{\mathrm{T}}\right]^{\mathrm{T}}, \\ \bar{\mathbf{a}}_{\mathrm{d}}^{(3)} &\triangleq \left[\bar{\mathbf{a}}_{\mathrm{d},2}^{\mathrm{T}}, \bar{\mathbf{a}}_{\mathrm{d},3}^{\mathrm{T}}, -\bar{\mathbf{a}}_{\mathrm{d},0}^{\mathrm{T}}, -\bar{\mathbf{a}}_{\mathrm{d},1}^{\mathrm{T}}\right]^{\mathrm{T}}, \\ \bar{\mathbf{a}}_{\mathrm{d}}^{(4)} &\triangleq \left[\bar{\mathbf{a}}_{\mathrm{d},3}^{\mathrm{T}}, -\bar{\mathbf{a}}_{\mathrm{d},2}^{\mathrm{T}}, \bar{\mathbf{a}}_{\mathrm{d},1}^{\mathrm{T}}, -\bar{\mathbf{a}}_{\mathrm{d},0}^{\mathrm{T}}\right]^{\mathrm{T}}. \end{aligned} \tag{35}$$

Based on the above real-valued vectors and matrix, (32) and (33) can be respectively changed into the SOC forms as

$$\begin{aligned} \min_{\breve{\mathbf{w}},\xi} \xi \quad \text{s.t.} \quad &\|\breve{\mathbf{Q}}\breve{\mathbf{w}}\| \leq \xi,\ \varepsilon\|\breve{\mathbf{w}}\| \leq \breve{\mathbf{w}}^{\mathrm{T}}\bar{\mathbf{a}}_{\mathrm{d}}^{(1)} - 1, \\ &\breve{\mathbf{w}}^{\mathrm{T}}\bar{\mathbf{a}}_{\mathrm{d}}^{(2)} = 0,\ \breve{\mathbf{w}}^{\mathrm{T}}\bar{\mathbf{a}}_{\mathrm{d}}^{(3)} = 0,\ \breve{\mathbf{w}}^{\mathrm{T}}\bar{\mathbf{a}}_{\mathrm{d}}^{(4)} = 0, \end{aligned} \tag{36}$$

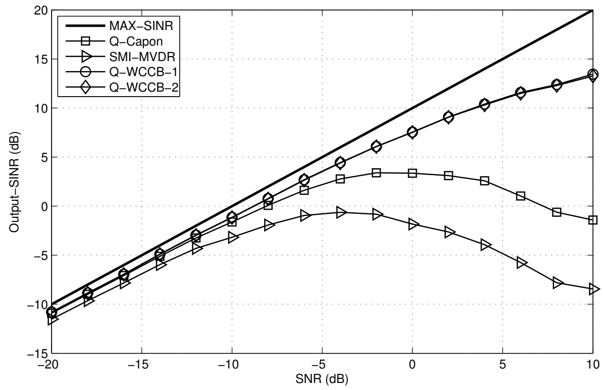

Fig. 2. Output SINR versus input SNR with a fixed sample size 100.

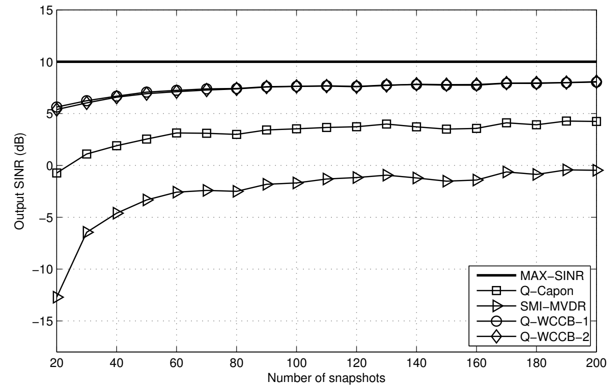

Fig. 3. Output SINR versus sample size with input SNR $= 0$ dB.

and

$$\min_{\breve{\mathbf{w}},\xi} \xi \quad \text{s.t.} \quad \|\breve{\mathbf{Q}}\breve{\mathbf{w}}\| \leq \xi,\ \varepsilon\|\breve{\mathbf{w}}\| \leq \breve{\mathbf{w}}^{\mathrm{T}}\bar{\mathbf{a}}_{\mathrm{d}}^{(1)} - 1. \tag{37}$$

By solving the above constrained minimization problems, the optimum real-valued weight vector $\breve{\mathbf{w}} \in \mathbb{R}^{4N\times 1}$ is obtained. The optimum quaternionic weight vector $\mathbf{w}_{\mathrm{Q-WCBB}} \in \mathbb{H}^{N\times 1}$ can then be obtained by re-arranging the elements of $\breve{\mathbf{w}}$ according to (34) and (35).

3. SIMULATIONS

In our simulations, we consider a ULA consisting of 10 crossed-dipoles spaced half a wavelength apart. In all examples, one desired signal along with two uncorrelated interferences is assumed to impinge upon the array from the $y - z$ plane with a fixed signal-to-interference ratio (SIR) of -10 dB. The DOAs of the interferences are fixed at 30° and 60°. For each scenario, 200 independent runs are used to calculate each simulation result. Four methods are compared in terms of average output SINR: the two proposed algorithms Q-WCCB-1 and Q-WCCB-2, the SMI-MVDR beamformer [17], and the Q-Capon beamformer [15]. In addition, the maximally achievable SINR denoted by 'MAX-SINR' is also displayed in the simulation results as a benchmark, which is obtained by the Q-Capon beamformer without steering vector error. The MATLAB toolboxes SeDuMi and YALMIP [20, 21], are employed to calculate the optimum weight vector of our robust beamformers.

In the first example, the output SINR versus the input SNR as well as the sample size are considered. The actual DOAs and polarizations of the signals are given as: $(\theta_{\mathrm{d}}, \gamma_{\mathrm{d}}, \eta_{\mathrm{d}}) = (5^\circ, 15^\circ, 30^\circ)$, $(\gamma_{\mathrm{i},1}, \eta_{\mathrm{i},1}) = (30^\circ, 80^\circ)$, and $(\gamma_{\mathrm{i},2}, \eta_{\mathrm{i},2}) = (70^\circ, 100^\circ)$. The norm of the mismatch error vector $\|\mathbf{e}\|$ is assumed to have a uniform distribution in the interval $(0, \varepsilon]$, where ε is fixed to 2 in this example. The results are given in Figs. 2 and 3. We can observe that the proposed methods consistently enjoy the best performance in terms of robustness and convergence rate, and their superiority is especially prominent in the case of high SNR values and small sample sizes. Additionally, the two proposed beamformers have almost the same performance in this simulation.

In our second example, the output SINR is studied as a function of the error constraint ε, which is varied from 0.6 to 3. The input SNR and sample size are 0 dB and 200, respectively. The actual DOAs and polarizations of signals are kept the same as in the first example. The performance of our quaternionic robust adaptive beamformers versus ε is shown in Fig. 4. The results demonstrate that Q-WCCB-1 is better than Q-WCCB-2 for small values of ε. When the value of ε is greater than about 1.8, Q-WCCB-2 has achieved a little better performance than Q-WCCB-1. Furthermore, the curves of Q-WCCB-1 and Q-WCCB-2 both decrease when ε is too large (greater than about 2.2).

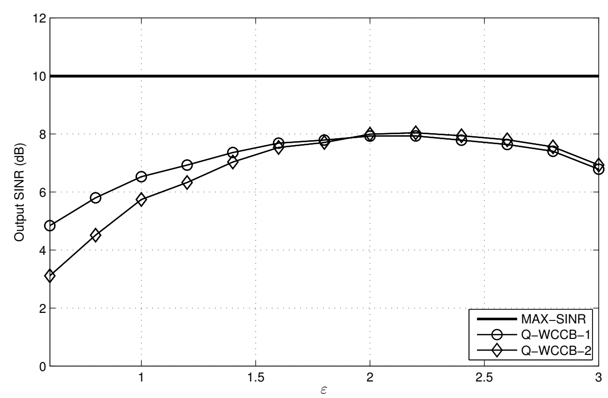

Fig. 4. Output SINR versus ε.

4. CONCLUSION

Based on the worst-case performance constraint, a novel adaptive beamforming scheme based on a two-component EM vector-sensor array has been proposed within the hypercomplex framework, and two adaptive algorithms are derived accordingly. They consistently outperform the recently proposed quaternionic adaptive beamformer Q-Capon as well as the traditional SMI-MVDR beamformer, especially in the circumstance of high input SNR values and small sample sizes. Additionally, the two algorithms show a very close performance in our numerical simulations.

5. REFERENCES

[1] R. T. Compton, "On the performance of a polarization sensitive adaptive array," *IEEE Transactions on Antennas and Propagation*, vol. 29, no. 5, pp. 718–725, September 1981.

[2] R. T. Compton, "The tripole antenna: An adaptive array with full polarization flexibility," *IEEE Transactions on Antennas and Propagation*, vol. 29, no. 6, pp. 944–952, November 1981.

[3] A. Nehorai, K. C. Ho, and B. T. G. Tan, "Minimum-noise-variance beamformer with an electromagnetic vector sensor," *IEEE Transactions on Signal Processing*, vol. 47, no. 3, pp. 601–618, March 1999.

[4] Y. G. Xu, T. Liu, and Z. W. Liu, "Output SINR of MV beamformer with one EM vector sensor of and magnetic noise power," in *IEEE International Conference on Signal Processing (ICSP)*, September 2004, vol. 1, pp. 419–422.

[5] J. Li and P. Stoica, Eds., *Robust Adaptive Beamforming*, John Wiley & Sons, Hoboken, New Jersey, 2005.

[6] S. A. Vorobyov, A. B. Gershman, and Z. Q. Luo, "Robust adaptive beamforming using worst-case performance optimization via second-order cone programming," in *IEEE International Conference on Acoustics, Speech, and Signal Processing (I-CASSP)*, May 2002, vol. 3, pp. III–2901–III–2904.

[7] S. A. Vorobyov, A. B. Gershman, and Z. Q. Luo, "Robust adaptive beamforming using worst-case performance optimization: A solution to the signal mismatch problem," *IEEE Transactions on Signal Processing*, vol. 51, no. 2, pp. 313–324, Febuary 2003.

[8] L. Yu, W. Liu, and R. J. Langley, "Robust beamforming with combined worst-case performance optimization and soft constraints in a multipath environment," in *Proc. European Signal Processing Conference*, Glasgow, Scotland, August 2009, pp. 583–586.

[9] L. Yu, W. Liu, and R. J. Langley, "A novel robust beamformer based on sub-array data subtraction for coherent interference suppression," in *Proc. IEEE Workshop on Statistical Signal Processing*, Cardiff, UK, September 2009, pp. 525–528.

[10] L. Yu, W. Liu, and R. J. Langley, "Robust beamforming methods for multipath signal reception," *Digital Signal Processing*, vol. 20, pp. 379–390, March 2010.

[11] L. Yu, W. Liu, and R. J. Langley, "Novel robust beamformers for coherent interference suppression with DOA estimation errors," *IET Microwaves, Antennas and Propagation*, vol. 4, pp. 1310–1319, September 2010.

[12] Y. Zhao and W. Liu, "Robust wideband beamforming with frequency response variation constraint subject to arbitrary norm-bounded error," *IEEE Transactions on Antennas and Propagation*, vol. 60, no. 5, pp. 2566–2571, May 2012.

[13] S. Miron, N. L. Bihan, and J. I. Mars, "High resolution vector-sensor array processing using quaternions," in *IEEE/SP 13th Workshop on Statistical Signal Processing*, July 2005, pp. 918–923.

[14] S. Miron, N. L. Bihan, and J. I. Mars, "Quaternion-MUSIC for vector-sensor array processing," *IEEE Transactions on Signal Processing*, vol. 54, no. 4, pp. 1218–1229, April 2006.

[15] X. M. Gou, Y. G. Xu, Z. W. Liu, and X. F. Gong, "Quaternion-Capon beamformer using crossed-dipole arrays," in *IEEE International Symposium on Microwave, Antenna, Propagation, and EMC Technologies for Wireless Communications (MAPE)*, November 2011, pp. 34–37.

[16] J. W. Tao and W. Chang, "The MVDR beamformer based on hypercomplex processes," in *IEEE International Conference on Computer Science and Electronics Engineering (ICCSEE)*, March 2012, vol. 2, pp. 273–277.

[17] J. W. Kim and C. K. Un, "An adaptive array robust to beam pointing error," *IEEE Transactions on Signal Processing*, vol. 40, no. 6, pp. 1582–1584, June 1992.

[18] N. L. Bihan and J. I. Mars, "Singular value decomposition of quaternion matrices: A new tool for vector-sensor signal processing," *Signal Processing*, vol. 84, no. 7, pp. 1177–1199, 2004.

[19] F. Zhang, "Quaternions and matrices of quaternions," *Linear Algebra and its Applications*, vol. 251, no. 0, pp. 21–57, 1997.

[20] J. F. Sturm, "Using SeDuMi 1.02, a MATLAB toolbox for optimization over symmetric cones," 1998.

[21] J. Lofberg, "YALMIP: A toolbox for modeling and optimization in MATLAB," in *IEEE International Symposium on Computer Aided Control Systems Design*, September 2004, pp. 284–289.